Solid State Communications 252 (2017) 6–10

Contents lists available at ScienceDirect

Solid State Communications

journal homepage: www.elsevier.com/locate/ssc

Communication

First principles study of crystal Si-doped $Ge_2Sb_2Te_5$

Beibei Yan, Fei Yang*, Tian Chen, Minglei Wang, Hong Chang, Daoming Ke, Yuehua Dai

School of Electronics and Information Engineering, Anhui University, Hefei 230601, China

ARTICLE INFO

Keywords:
GST
First-principles
Si-doping
Doping concentration

ABSTRACT

$Ge_2Sb_2Te_5$ (GST) and Si-doped GST with hexagonal structure were investigated by means of First-principles calcucations. We performed many kinds of doping types and studied the electronic properties of Si-doped GST with various Si concentrations. The theoretical calculations show that the lowest formation energy appeared when Si atoms substitute the Sb atoms (Si_{Sb}). With the increasing of Si concentrations from 10% to 30%, the impurity states arise around the Fermi level and the band gap of the Si_{Sb} structure broadens. Meanwhile, the doping supercell has the most favorable structure when the doping concentration keeps in 20%. The Si-doped GST exhibits p-type metallic characteristics more distinctly owing to the Fermi level moves toward the valence band. The Te p, d-orbitals electrons have greater impact on electronic properties than that of Te s-orbitals.

1. Introduction

Phase-change random access memory (PCRAM) is one of the attractive memories due to its non-volatile, high speed, small size and compatible with CMOS technology well [1]. Memory processes are based on revisable phase transition between amorphous and crystalline states of storage materials [1–3]. The amorphous states is created by pulse to melt the material and then cool down quickly, while the crystalline states is achieved by heating the material above the crystallization temperature but below the melting point [1,2].

PCRAM generally refers to the chalcogenide-random access memory [2]. As the chalcogenide material, GST has recently demonstrated outstanding performance and is being considered as one of the most promising candidates for the next generation memory materials [4]. Structure of the GST reported in papers mainly points metastable cubic and more stable hexagonal [3]. There are three kinds of sequence models about hexagonal GST: the layer sequence of -Te-Ge-Te-Sb-Te-Te-Sb-Te- Ge- presented by Kooi and De Hosson (K-DH model) [5], interchange Ge and Sb layer by Petrov et al. (Petrov model) [6] and the Te wholly occupies the sublattice and the cations (Ge, Sb) randomly occupy in the same layer proposed by Matsunaga et al. (Matsunaga model) [7].

Recently, studies on the defects about GST are more and more remarkable. For example, both the antisite defective(Te atoms at Sb sites (Te_{Sb}) and Sb atoms at Te sites (Sb_{Te})) are proved energetically favorable and mechanistically stable in GST alloys [3], the vacancies in structured GST are also existed and electrical properties of GST have been studied [8–15]. Cu-doped in the amorphous structure of GeTe was also performed and reveals that the coordination environment changes result in the incorporation of Cu [16]. In our experiments, Si atoms were doped into the crystal structure of GST by substitutional doping and interstitial doping (Si_i) to improve the electrical properties and reduce the power consumption. The formation energy of the Si atom substitute Ge atom (Si_{Ge}), the Si atom substitute Sb atom (Si_{Sb}), the Si atom substitute Te atom (Si_{Te}) and Si_i have been calculated, respectively. Meanwhile, Si-doped GST structures with different doping concentrations were studied.

2. Materials and methods

All calculations were performed using the Vienna *ab initio* simulation package (VASP) [17]. The plane wave pseudo potential method was adopted to describe the electronic structure of molecular dynamics and the First-principles. The exchange correlation of electrons is treated with the generalized gradient approximation (GGA) [18].

A plane wave basis with a cutoff energy of 300 eV was used. The model for calculation of band structures has 9 atoms, and the ratio of Ge:Sb:Te was 2:2:5. The lattice parameters are a=4.2247 Å, b=4.2247 Å and c=17.2391 Å. Meanwhile, 5×1×1 supercell model for crystallize GST was used to calculate TDOS distinctly, we expanded single cell five times in the x direction, and the supercell of crystalline hexagonal structure include 10 Ge atoms, 10 Sb atoms, 25 Te atoms. The lattice parameters are a=21.1235 Å, b=4.2247 Å, c=17.2391 Å.

The structure of Si_{Sb} was proposed to discuss the different concentrations effects of Si doping on crystalline GST. We also discussed the influence of different orbits (s, p, d) on the electronic

* Corresponding author.
E-mail addresses: 543194576@qq.com (B. Yan), feiyang-0551@163.com (F. Yang), 1354654460@qq.com (T. Chen), 2628253966@qq.com (M. Wang), 814874822@qq.com (H. Chang), kedaoming@sohu.com (D. Ke), 1097683210@qq.com (Y. Dai).

http://dx.doi.org/10.1016/j.ssc.2017.01.001
Received 16 November 2016; Received in revised form 21 December 2016; Accepted 4 January 2017
Available online 05 January 2017

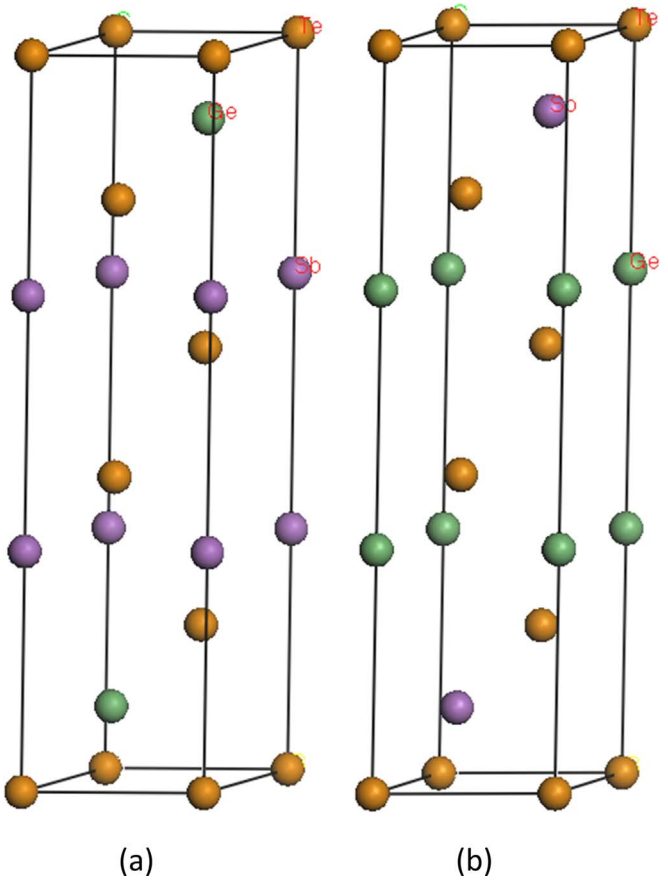

Fig. 1. (Color online) The layer sequences structure in hexagonal phase GST of (a) K-DH model and (b) Petrov model. The green, purple and brown balls denote Ge, Sb and Te atoms, respectively.

properties. In our experiments, 1×5×1 k-points were used during the structure optimization and 1×5×2 k-points were adopted for examining the electronic properties. The calculation of band structure sets the Brillouin zone path as the k-points. The TDOS, The partial density of states (PDOS), and band structure was handled by Origin [19].

3. Results and discussion

The structures of GST with the K-DH model and the Petrov model were displayed in the Fig. 1.

As shown in Fig. 1, comparing the two kinds of structure, Te atoms occupying sites were unchanged while the sites of Ge atoms and Sb atoms were exchanged. The previous studies show that the K-DH model has the lower cohesive energy that is 6 meV/atom lower than the Petrov model, therefore the K-DH structure was used in this work [3].

We performed the total energies of Ge, Sb, Te, Si atom and the crystalline GST with K-DH model about different doping types, the results were shown in the first line of Table 1.

The amount of the formation energy reveals the difficult level of defect formation, the stability of defect system. When the model is built for the $Si_{Ge/Sb/Te}$, the the atoms (Ge/Sb/Te) were replaced by Si atoms. While the Si_i model was obtained by doping the Si atom interstitially. The formation energy was calculated according to the following Eq. (1)

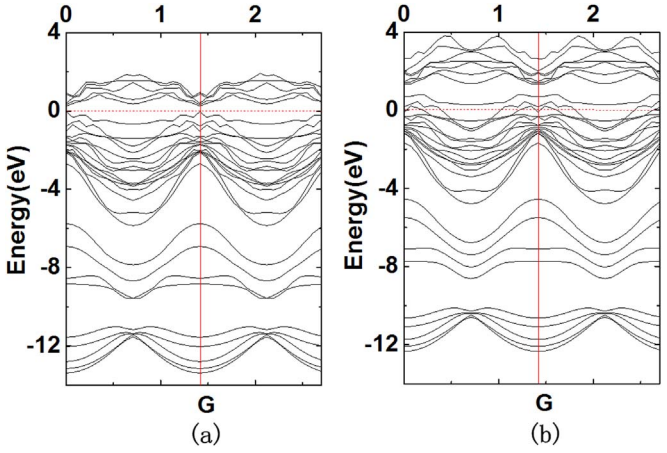

Fig. 2. (Color online) The calculated band structures with the layer sequences of (a) GST structure and (b) Si-doped GST structure, where the Fermi level is set at 0 eV.

[20]:

$$E_f = E_{Si-doped} - E_{GST} - n(E_{Si} - E_V) \quad (1)$$

where E_f is formation energy of defects, $E_{Si\text{-}doped}$ is total energy of Si-doped GST, E_{GST} is energy of crystalline hexagonal GST, E_{Si} is energy of single Si atom, E_V is the energy of single atom (Ge/Sb/Te) which is replaced by Si atom and n stand for the number of replaced Si atoms. The formation energies are shown in the second line of Table 1. We can get that Si_{Sb} structure has the lowest formation energy by comparison, which is 0.213 eV lower than Si_{Ge} structure, 0.725 eV lower than Si_{Te} structure and 1.099 eV lower than Si_i structure. It is noted that Si_{Sb} structure is energetically favorable to form and this structure was used in the later experiments.

The single cells of GST and Si-doped GST were adopted to acquire band structure, the calculated results of band structures are shown in Fig. 2. The energy level of each atom is represented in the graph, the horizontal axis is k-points, the vertical axis is energy and G is the higher symmetry point which is the center of the wave.

As seen from Fig. 2, the bottom of the conduction band and the top of valence band occur at the same k, this means that GST is a direct band gap material and the electron transition from valence band to conduction band just need to absorb energy. Compared to GST, Si-doped GST exhibits p-type metallic behavior more distinctly because the Fermi level moves toward the valence band. The band gap of GST and Si-doped GST are 0.25 eV and 0.75 eV, respectively. There are 0.5 eV increasing of the band gap, two acceptor levels appeared in the conduction band which is obviously caused by the doping Si atoms. The band structure of the Si-doped GST moved toward higher energy about 1 eV, then the electronic transition becomes difficult and the carrier concentration reduced in a certain extent. Moreover, the resistivity increased with Si doping, power consumption reduced and the ability to maintain data improved. All the above results suggest that Si doping can improve the electrical properties of GST effectively.

To calculate the TDOS, 5×1×1 supercell with 45 atoms was used. To obtain different concentrations (10%, 20%, 30%) of doping, we replaced 1, 2, 3 Sb atoms with Si atoms respectively. The total densities of states (TDOS) of various types Si-doped GST were shown in Fig. 3.

As we can see from Fig. 3, the strong contact of the electronic properties with Si doping are displayed as follows: (i) after doping, the

Table 1
The total energies E_{tot} (eV) of structures for relevant single atoms and polycrystalline and the formation energies E_f (eV) for Si-doped GST structure with various doping types.

	Ge	Sb	Te	Si	GST	Si_{Ge}	Si_{Sb}	Si_{Te}	Si_i
E_{tot}(eV)	−4.263	−4.225	−3.211	−5.404	−33.880	−34.238	−34.489	−34.777	−36.928
E_f(eV)	–	–	–	–	–	0.783	0.570	1.295	2.356

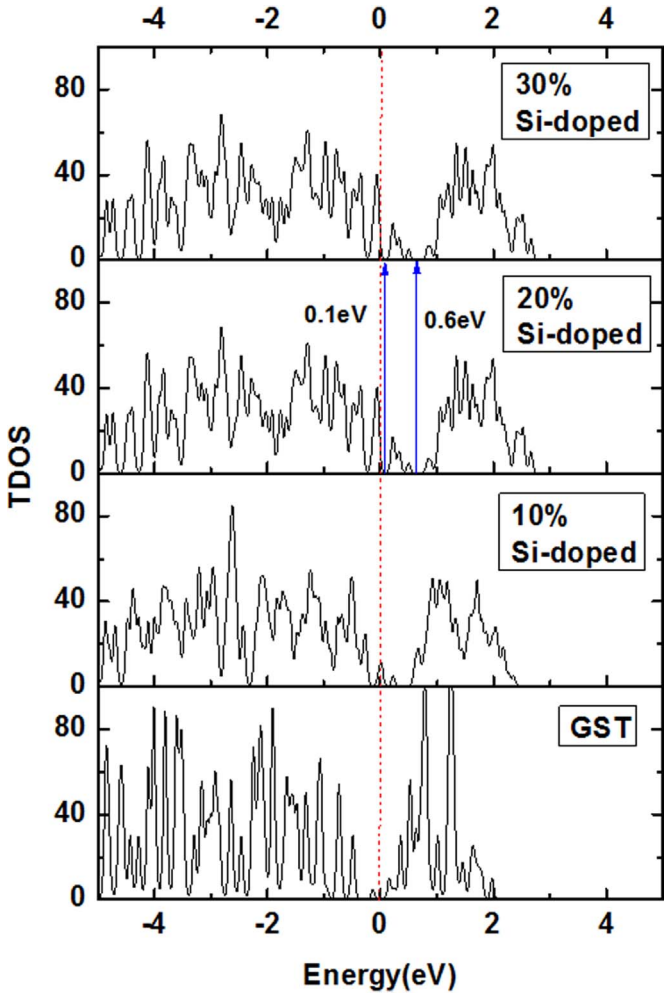

Fig. 3. TDOS for crystal GST, 10%, 20% and 30% Si doping concentrations crystal GST. The Fermi level is set at 0 eV.

peaks intensity of conduction band and valence band increased significantly; (ii) with the Si doping concentrations from 10% to 30%, the impurity states appeared around the Fermi level which is located near the top of the valence band. These impurity states originated from the Si atoms; (iii) by comparing the TDOS of Si-doped GST with 10–20% concentrations, the impurity states and conduction band become more and more widen with the increasing of doping concentrations; (iv) there is no difference on TDOS of Si-doped GST by comparing 20–30% doping concentrations; (v) in Fig. 3, Si-doped impurity states appeared in the band gap region when the doping concentration is 20%, it is located at 0.6 eV below the conduction band and 0.1 eV above the valence band [21,22], which is caused by the Si doping obviously.

In conclusion, we can get that when the Si-doping concentrations below 20%, the impurity states become wider and the peaks intensity of the TDOS increase with the increasing of the doping concentration. However, once the doping concentration increases over than 20%, the TDOS has no change distinctly. In other words, the 20% concentrations Si-doped GST is the most effective structure. So the following studies are based on the 20% concentrations Si doping GST.

In the 20% concentrations doping structure, 2 Sb atoms were replaced by Si atoms. Because there are 10 Sb atoms in the supercell, the electronic properties of Si-doped GST are supposed to vary site by site of doping. We just selected four kinds in many doping situations to calculate the TDOS, the results are shown in Fig. 4 as 1#, 2#, 3# and 4#.

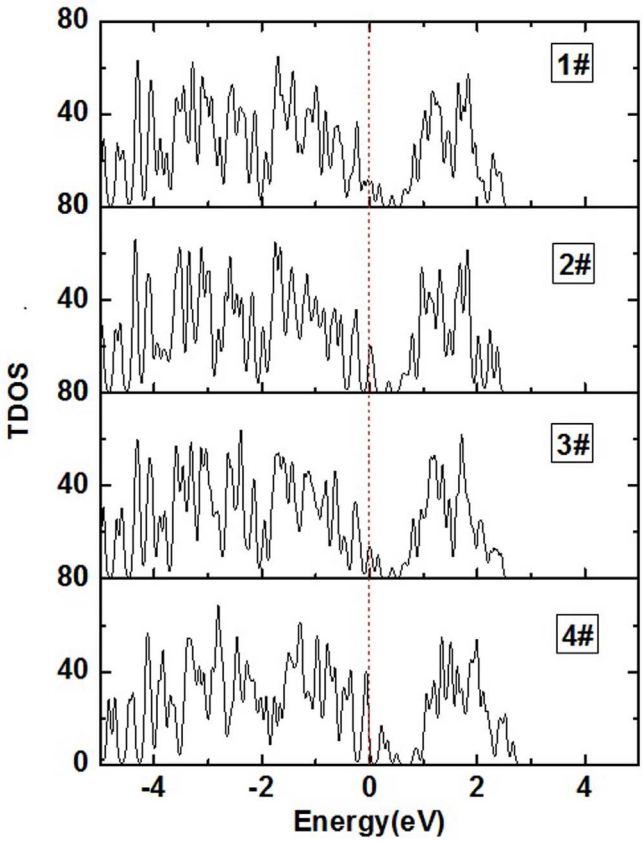

Fig. 4. The TDOS of GST with different doping sites as 1#, 2#, 3# and 4#.

According to the Fig. 4, we can see that the trend of the TDOS is basically consistent in the four cases; meanwhile the peaks of the valence band and conduction band are also the same. These indicate that the location of the doping atoms does not affect the electronic properties of the whole system.

Another significant issue is the effect of each atom on electronic properties, and then PDOS of atom were also calculated. As seen in the Fig. 5, the PDOS of the atom with the structure of Si-doped GST moves towards higher energy, which is consistent with the trend of TDOS.

As the Si-doped GST exhibits p-type metallic behavior more distinctly, the hole concentration in the semiconductor is much larger than electron concentration. So we mainly consider the conductive properties of the valence band. A comparison between Fig. 5 obviously reveals that the peaks in valance band of Te PDOS (shown in Fig. 5(c)) are higher than that of other atoms (shown in Fig. 5(a), (b) and (d)), these results can show that Te atoms play a major role to the valence band of the TDOS. Meanwhile, the Te p, d orbitals PDOS have higher peaks which illustrate that the Te p, d-orbitals electrons have greater impact on electronic properties than that of Te s-orbitals.

4. Conclusions

We have studied the structure of Si-doped GST based on the *ab initio* calculations. Among the many kinds of doping types, the Si_{Sb} structure which has the lowest formation energy is considered to be most easily formed. Comparing the band structure of GST with the Si-doped GST, we found that the Si-doped GST structure has higher energy, wider conduction band and band gap. These changes will contribute to the decreasing power consumption, the ability to maintain data improved and the expansibility increased. By comparing

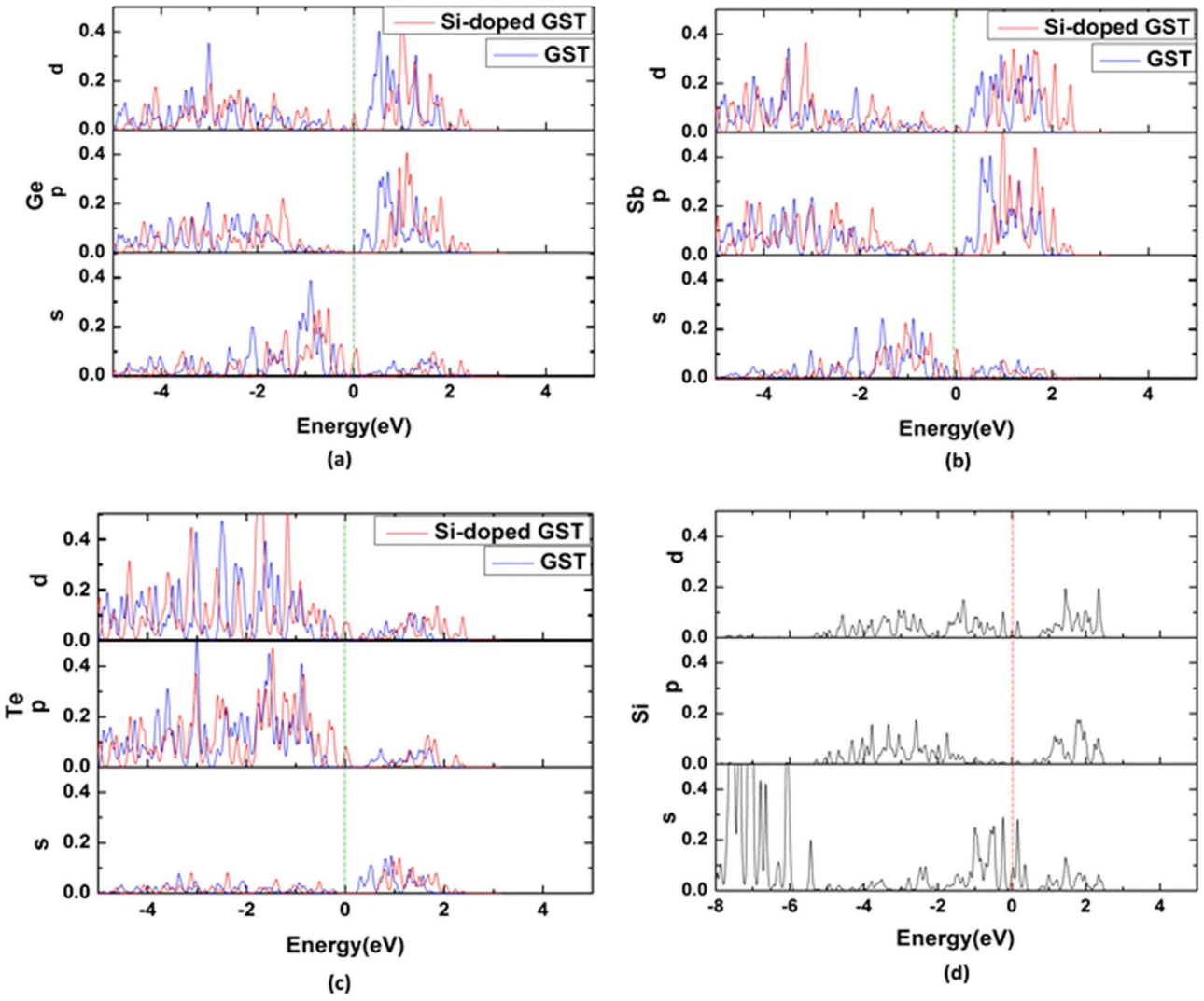

Fig. 5. (Color online) The PDOS (s, p, d orbitals) of (a) Ge atom, (b) Sb atom and (c) Te atom before and after doping. The blue and red lines denote GST and Si-doped GST, respectively. (d) The PDOS (s, p, d orbitals) of Si atom. The Fermi level is set at 0 eV.

different doping concentrations, 20% of the doping concentration is the most effective while the location of the doping is ineffective. The structure exhibits p-type metallic behavior more distinctly owing to the Fermi level moves to the valence band. The Te p, d-orbitals electrons have greater impact on electronic properties than that of Te s-orbitals. We expect that these findings may contribute to the phase-change community.

Acknowledgments

This work is supported by the National Natural Science Foundation of China (Grant no. 61376106), Natural Science Foundation of the Higher Education Institutions of Anhui Province (Grant no. KJ2016A035) , the Doctoral Scientific Research Starting Foundation of Anhui University (Grant no. J10113190025) and Graduate Innovation Foundation of Anhui University (Grant no. yqh100164). Besides, all the numerical calculations in this paper have been done with the help of the Supercomputing Center of Anhui University of China.

References

[1] Geunsik Lee, Seung-Hoon Jhi, Ab initio studies of structural and electronic properties of the crystalline $Ge_2Sb_2Te_5$, Phys. Rev. B 77 (2008) 153201.
[2] S. Cararati, M. Bernasconi, T.D. Kvhne, M. Krack, M. Parrinello, First-principles study of crystalline and amorphous $Ge_2Sb_2Te_5$ and the effects of stoichiometric defects, J. Phys.: Condens. Matter 22 (2010) 399801.
[3] Jian Zhou, Zhemei Sun, Yuanchun Pan, Zhitang Song, Rajeev Ahuja, Ab initio study of antisite defective layered $Ge_2Sb_2Te_5$, Mater. Chem. Phys. 133 (2012) 159–162.
[4] Noboru Yamada, Toshiyuki Matsunaga, Structure of laser-crystallized $Ge_2Sb_{2+x}Te_5$ sputtered thin films for use in optical memory, J. Appl. Phys. 88 (2000) 7020–7028.
[5] B.J. Kooi, J. Th.M. De Hosson, Electron diffraction and high-resolution transmission electron microscopy of the high temperature crystal structures of $Ge_xSb_2Te_{3+x}$ (x=1, 2, 3) phase change material, J. Appl. Phys. 92 (2002) 3584–3590.
[6] I.I. Petrov, R.M. Imamov, Z.G. Pinsker, Electron-diffraction determination of the structures of $Ge_2Sb_2Te_5$ and $GeSb_4Te_7$, Sov. Phys. Crystallogr. 13 (1968) 339.
[7] T. Matsunaga, N. Yamada, Y. Kabota, Acta Crystallogr, Structures of stable and metastable $Ge_2Sb_2Te_5$, an intermetallic compound in GeTe-Sb_2Te_3 pseudobinary systems, Acta Crystallogr. Sect. B: Struct. Sci. 60 (2004) 685–691.
[8] S. Senkader, C.D. Wright, Models for phase-change of $Ge_2Sb_2Te_5$ in optical and electrical memory devices, J. Appl. Phys. 95 (2) (2004) 504–511.
[9] J. Zhou, Z. Sun, Y. Pan, Z. Song, R. Ahuija, Vacancy or not: An insight on the intrinsic vacancies in rocksalt-structured GeSbTe alloys from ab initio calculations, EPL 95 (2011) 27002.
[10] R. Pandian, B.J. Kooi, G. Palasantzas, J.T.M. De Hosson, Reversible Electrical Resistance Switching in GeSbTe Thin Films: An Electrolytic Approach without Amorphous-Crystalline Phase-Change, Mrs Online Proceedings Library, 2008, p. 1071.
[11] Y.J. Park, J.Y. Lee, M.S. Youm, Y.T. Kim, H.S. Lee, Crystal structure and atomic arrangement of the metastable $Ge_2Sb_2Te_5$ thin films deposited on SiO_2/Si substrates by sputtering method, J. Appl. Phys. 97 (9) (2005) 093506.
[12] Naihua Miao, Baisheng Sa, Jian Zhou, Lihua Xu, Zhimei Sun, Rajeev Ahuja, Investigation on $Ge_{5-x}Sb_xTe_5$ phase-change materials by first-principles method,

Appl. Phys. A 99 (4) (2010) 961–964.
[13] Zhimei Sun, Amorphous structure melt-quenched from defective $Ge_2Sb_2Te_5$, J. Mater. Sci. 47 (21) (2012) 7635–7641.
[14] Baisheng Sa, Zhimei Sun, Electron interactions and Dirac fermions in grapheme-$Ge_2Sb_2Te_5$ superlattices, J. Appl. Phys. 115 (23) (2014) 233714.
[15] Baisheng Sa, Jian Zhou, Rajeev Ahuja, Zhimei Sun, First-principles investigations of electronic and mechanical properties for stable $Ge_2Sb_2Te_5$ with van der Waals corrections, Comput. Mater. Sci. 82 (2014) 66–69.
[16] Linchuan Zhang, Baisheng Sa, Jian Zhou, Zhitang Song, Zhimei Sun, Atomic scale insight into the amorphous structure of Cu doped GeTe phase-change material, J. Appl. Phys. 116 (15) (2014) 153501.
[17] G. Kresse, J. Hafner, Ab initio molecular dynamics for liquid metals, Phys. Rev. B 47 (1993) 558–561.
[18] J.P. Perdew, Y. Wang, Accurate and simple analytic representation of the electron-gas correlation energy, Phys. Rev. B 45 (23) (1992) 13244–13249.
[19] Gastón Darío Pierinia, David Douglas Sousa Fernandesb, Paulo Henrique Gonçalves Dias Dinizc, Mário César Ugulino de Araújob, María Susana Di Nezio, María Eugenia Centurión, A digital image-based traceability tool of the geographical origins of Argentine propolis, Microchem. J. 128 (2016) 62–67.
[20] G. Grimvall, Thermophysical Properties of Materials, Elsevier, 1999.
[21] Bo Xiao, Tingkun Gu, Tomofumi Tada, Satoshi Watanabe, Conduction paths in Cu/amorphous-Ta_2O_5/Pt atomic switch: First-principles studies, J. Appl. Phys. 115 (3) (2014) 034503.
[22] Bo Xiao, Satoshi Watanabe, Oxygen vacancy effects on an amorphous-TaO_x-based resistance switch: a first principles study, Nanoscale 6 (2014) 10169–10178.